

# Finite Element Analysis of Connecting Rod to determine the Critical Buckling Stress and Factor of Safety

Sourabh Jain<sup>1</sup>, Prof. Pradyumna Viswakarma<sup>2</sup>

<sup>1</sup>(M.Tech Industrial Design, Radharaman Institute of Research & Technology. Bhopal, India)

<sup>2</sup>(Professor Mechanical Engineering, Radharaman Institute of Research & Technology. Bhopal, India)

**Abstract** – In our analysis, ANSYS was used and the model was developed on UniGraphics. In order to verify the present ANSYS model, the critical buckling with their deformation by using C70S6 material are compared with the available experimental results present in the literature. And the design of connecting rod with different middle thickness (5.5,5.4,5.3,5.2,5.1) & side width (6.0,6.1,6.2,6.3,6.4). In this study, the simulations of different middle thickness & side width, was analyzed for factor of safety and the configurations of connecting rod are proposed. The results show that increasing side width and decreasing middle thickness increases radius of gyration and factor of safety for each location of connecting rod and decreases the slenderness ratio with increase in a side width simultaneously. The factor of safety of the connecting rod is compared by using four types of profiles i.e. middle thickness (5.5,5.4,5.3,5.2,5.1) & side width (6.0,6.1,6.2,6.3,6.4) of optimized connecting rod for various location.

**Keywords** – Connecting Rod, Factor of Safety, Critical Buckling, Allowable Stress, Finite Element Method.

## I. INTRODUCTION

In a reciprocating piston engine, the connecting rod connects the piston to the crank or crankshaft. In modern automotive internal combustion engines, the connecting rods are most usually made of structural steel for heavy engines, but can be made of aluminum for light weight high strength, durability or titanium (for a combination of strength and durable at the expense of affordability) for high output performance engines, or of cast iron for applications like scooters mopeds etc.. The small end attaches to the wrist pin, which is currently most often press fit into the connecting rod. The connecting rod is under huge amount of stress from the reciprocating load exerted by the piston, actually tearing and being compressed with every cyclic motion, and the load increases to the peak power with increasing engine acceleration. Failure of a connecting rod, usually called "throwing a rod" is one of the most common causes of catastrophic engine failure in cars, frequently putting the broken rod through the side of the crankcase and thereby rendering the engine irreparable; it can result from fatigue near a physical defect in the rod, lubrication deficiency in a bearing due to low maintenance or from failure of the rod bolts from a defect, improper fastening, or used of less strength bolts where not recommended. Despite their frequent occurrence on televised competitive automobile events, such failures are quite rare on production cars during normal daily driving. This is because production auto parts have a much larger factor of safety.

## II TYPES OF CONNECTING ROD

**Aluminum Connecting Rods-** These are CNC machined out of their proprietary. Al alloys are cold extruded but a pair of, 1000 a lot of pressure to make sure consistent grain flow and density. Aluminum Connecting Rods are offered for many any import or domestic applications by providing a totally custom rod at very little or no value on top of that of an "off-the-shelf" product. To be use in high H.P. (1,200 max) and high rate (14,000 max) applications. Because of low fatigue life, once used below high stress things drag athletics solely. Are often use safely with daily driving. Al rods are the most effective alternative for DSM's, sturdy and lightweight.



Figure1.1 –Connecting rod made of Aluminum [26]

**Steel Connecting Rods-** Still connecting rods to be employed in moderate to high HP (Forged 900 max, Billet 1200 max) and moderate rate (9500-10,000 max). Appropriate for daily driving, endurance athletics, and drag athletics. Manufacturer makes the best quality steel I beam connecting rods for the DSM. They're appropriate for a multiplicity of applications. A special shot preening method will increase the fabric density on the part surface, leading to wonderful strength and sturdiness of the ultimate product, from OEM product to high-end race engines.



Figure1.2 –Connecting rod made of Steel [26]

**Titanium Connecting Rods-** metal connecting rods to be use in high power unit (1,400 max) and high revolutions per minute (14,000) applications. Maybe use in daily driving, endurance athletics, and drag athletics. Set the benchmark on racetracks round the world. Due to their low weight, they're notably appropriate for top speed Motorsports engines



Figure1.3 –Connecting rod made of Titanium [26]

### III. LITERATURE REVIEW

**H. Grass et.al [2006]** - during this investigation a piece items from all stages of the method are won't to examine the pure mathematics, microstructure and native mechanical properties. Combining the results of those examinations with data on native method variables like strain and temperature from numerical simulation created it doable to review the influence of the deformation history on the native microstructure and mechanical properties. The simulation of the new forming method shows sensible agreement with experiments concerning to pure mathematics and temperature fields of the piece of work.

**S. Griza et.al [2009]** - A finite component Analysis was performed in reference to an analytical fracture mechanics approach progressing to assess the relation between alteration force and fissure propagation in rod bolts. The engine collapse occurred owing to forming laps within the grooves of the bolt shank. Finally, some style enhancements were recommended for avoid future failures: a niche within the groove length at the rod cap interface, enough to avoid combination of forming laps and better stress amplitude; increase of the bolt force assembly to cut back stress amplitude.

**Moon Kyu Lee et.al [2010]** - The buckling stresses from the recommended FEA approach are nearer to those measured in rig experiments than those from classical formula are. The strain sensitivities to reduction of rod shank are then examined in lights of yield, fatigue and buckling. The strain sensitivity in buckling indicates to be comparatively on top of or similar to those of yield and fatigue. Consequently, once weight reduction of affiliation rod shank is tried, buckling ought to be thought of as a necessary issue in conjunction with the opposite criteria like yield and fatigue.

**Liming Zheng et.al [2010]** - it absolutely was found that the FEM simulations results showed sensible consistency with the experiments, that indicates that the finite component model is possible and reliable. supported the principal findings from the 2 strategies, optimum ranges of method parameters for various fracture cacophonous connecting rods were foretold, that are a flexibly adjusting notch depth, a curvature radius but zero.08mm and a gap angle among the vary 18–261. The results indicate that the predicting ranges are appropriate for creating sensible SNs that has additionally been proved by the fracture cacophonous experiments.

**Vanluu Dao et.al [2012]** - With the rise of applied squeeze pressure, the scale of a-Al particles decreases whereas the form issue will increase, that increase the mechanical properties of the connecting-rods. Once the running temperature and die temperature increase, the scale and form issue of primary a-Al particles increase .However, if the die temperature is on top of three hundred 1C, the form issue decreases suddenly. The simplest microstructure and mechanical properties of connecting-rods made-up by SSSC were obtained at the running temperature of 575 1C, die temperature of approximately250 1C, and squeeze pressure of 100MPa.

**Saharash Khare et.al [2012]** - the hundreds and boundary conditions obtained from the experiments were employed in the finite component model of the rod assembly. A result shows high surface pressure and stresses close to the junction of internet and rim of the rod. The changed style of the rod shows important reduction within the extreme pressure in FEM leading to the many improvement of sturdiness life in laboratory check. A discussion of the spalling drawback has been provided resulting in the affiliation of choose pressure and spalling phenomena.

**Xianghui Meng et.al [2012]** - The piston dynamics, the oil film and therefore the friction loss of the system square measure analyzed and compared with one earlier model that has been adopted wide. The results on a internal-combustion engine show that the rod inertia will have some influence on the system lubrication yet because the piston dynamics, particularly once engine runs at high speeds.

**S.B.Chikalthankar et.al[2012]**- Numerical tools are extraordinarily used throughout the rod development part, therefore, the entire perceive of the mechanisms concerned yet because the dependableness of the numerical methodology are extraordinarily necessary to require technological benefits, such as, to cut back project time interval and prototypes price reduction. This work shows the entire rod Finite component Analysis (FEA) methodology. It absolutely was additionally performed a fatigue study supported Stress Life (SxN) theory, considering the changed clarinetist diagram.

**Prof. N.P.Doshi et.al [2013]** - Ansys bench module had been used for analysis of rod. We have a tendency to recognize the stresses developed in rod below static loading with totally different loading conditions of compression and tension at crank finish and pin finish of rod. We've additionally styled the rod by machine design approach. Style of rod that by machine design approach is compared with actual production drawing of rod. We have a tendency to found that there's risk of more reduction in mass of rod.

**Bai-yan He et.al [2013]** - Hardness and tensile tests are performed to verify the mechanical properties of the rod. A nonlinear finite component (FE) analysis with the locked assembly is performed to judge the native stress close to the conjugation faces, and therefore the results shows that the crack position is in step with the high stress spots. As a result, lower yield strength of the fabric and high stress level or high stress concentration are terminated because the main reasons of failure of the rod.

**G. naga Malleshwara Rao et.al [2013]** - This was entailed by activity an in depth load analysis. Therefore, this study has treated two subjects, first, static load and stress analysis of the rod and second, style optimization for appropriate material to attenuate the deflection. Within the initial of the study the hundreds performing on the rod as a perform of your time square measure obtained. The relations for getting the hundreds

for the rod at a given constant speed of crank shaft also are determined. It may be over from this study that the rod may be designed and optimized underneath a comprising tensile load such as 3600 crank angle at the most engine speed in concert extreme load, and also the crank pressure because the alternative extreme load. What is more, the prevailing rod may be replaced with a replacement rod manufactured from Genetic Steel.

### Validation of the Experimental Result

The validation of the Experimental result is done by carrying out the simulation work on the ANSYS Static Structural and Linear Buckling (Coupled) 15.0 Work bench.

### Experimental and Simulation Result-

Critical buckling stress prediction- Classical buckling analysis

**Euler's formula-**

$$\left( \sigma_{cr}^e = \frac{\pi^2 E}{\frac{K_y L}{r_y}} \right)^2 \dots \dots \dots (1)$$

Where E is the elastic modulus,  $K_y$  is 0.5 for a fixed-fixed joint effective length L, radius of gyration r this formula is used to analyze classical buckling for symmetrical column

### Rankine formula

$$\sigma_{cr} = \left( \frac{1}{\sigma_{cr}^e} + \frac{1}{\sigma_{cr}^p} \right)^{-1} \dots \dots \dots (2)$$

Where is Euler formula, yield strength this formula is used to analyze classical Buckling for unsymmetrical column

### Buckling prediction via finite element analysis

$$\sigma_{fem} = \frac{\text{Load Multiplier} \times \text{Applied Static Load}}{\text{Area}} \dots \dots \dots (3)$$

### 4.2 Stress prediction via finite element analysis

Critical buckling is analyzed by Euler's formula but connecting rod is unsymmetric section a rankine formula is used to predict buckling stresses to validate the value of load multiplier is evaluated by finite element method from ANSYS workbench and critical buckling stresses are calculated by equation no. (3)

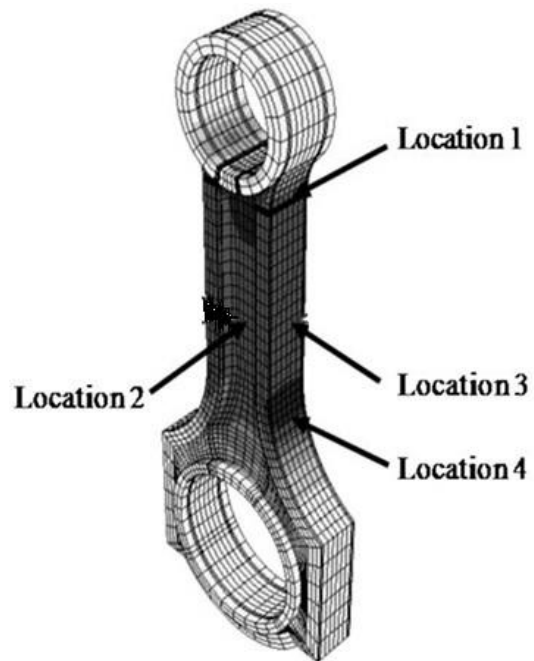


Fig- 4.1 Variable Location of connecting rod [3]

### Classification of connecting rod location for prediction of Allowable stress and to analyze Factor of Safety

Location - 1	Just below Small end edge
Location - 2	Middle of the side shank area
Location - 3	Middle of front I - Section flange area
Location - 4	Just top side edge of an big end

A variable location are used to determine the factor of safety at first the 64.7KN of static load is applied to a small end and allowable stresses values were analyzed with an strain gauge as in reference paper [Buckling sensitivity of a connecting rod to the shank sectional area reduction] [3].

### 4.3 Factor of Safety of connecting rod of different middle thickness & side width of shank cross section area

A static structural and linear buckling analysis (coupled) was carried out on C70S6 material connecting rod with different middle thickness & side width shank cross sectional area to determine the factor of safety and distribution of stresses along the effective length of the connecting rod. buckling stress distribution contours in case optimized connecting rod section area 26mm, 25mm, 24mm, 23mm, 22mm with different middle thickness & side width in each sectional area of connecting rod shank for the five different profiles are shown in Figures and the effect of different shank area profiles on the buckling stress distribution for various shank cross sectional area are represented in the Figures 4.3.

It is evident that there is a decrement in the slenderness ratio and gradually increase in radius of gyration due to optimizing the connecting rod section by providing a variable middle thickness & side width of connecting rod shank sectional area in a different profile of connecting rod a width of cross sectional area of shank is reduced by 1mm and cross section is



optimized by optimizing the parameters of cross section web ,on decreasing middle thickness and increasing side width of cross section radius of gyration increases due to this strength and durability increases but slenderness ratio decreases due to optimized side width of connecting rod cross sectional area of shank reduces stress concentration factor and increases factor of safety due to particle concentration in optimized-section is more than I-section ,Hence strength ,durability of connecting rod increases

$$\text{Factor of Safety} = \frac{\text{Ultimate Stress}}{\text{Allowable Stress}}$$

#### 4.4 Vonmises Stress Distribution at various location of connecting rod of Different shank cross section area

A static structural and linear (coupled) analysis was carried out on C70S6 material connecting rod to determine the vonmises stress distribution at different locations.

#### 4.5 Vonmises Stress distributions on side rear face of connecting rod of reduced shank sectional area-

Vonmises stress distribution contours in case of cross sectional area reduction for different profiles are shown in Figures 4.1. The effect of different profiles on the vonmises stress distribution various location are shown. From the Figures below, it can be seen that the nature of the vonmises stress is compressive. A stresses developed at different locations of connecting rod of reduced cross sectional area It is also observed that the magnitude of the stress is maximum in the optimized-section of a connecting rod compared to I-section it could be analyzed that optimized-section is more durable than I-section.

#### 4.6 Finite Element Model Validation -

##### 4.6.1Buckling stresses-

Result of buckling stress are obtained by FEM is compared with the buckling stress value calculated by the rankine formula as [3] are compared in the below table. The result shows the accuracy of the FEM which is similar to classical method for obtaining buckling stress.

Table-(4.1) Experimental and Simulation Result for the Reduced cross section of Connecting rod

Thickness (L1)	Reference Paper Rankine Formula Calculation Results[3]	Simulation Results	Percentage Error
26	568	609	7.2 %
25	564	602	6.7 %
24	561	591	5.3 %
23	554	584	5.4 %
22	552	581	5.3 %

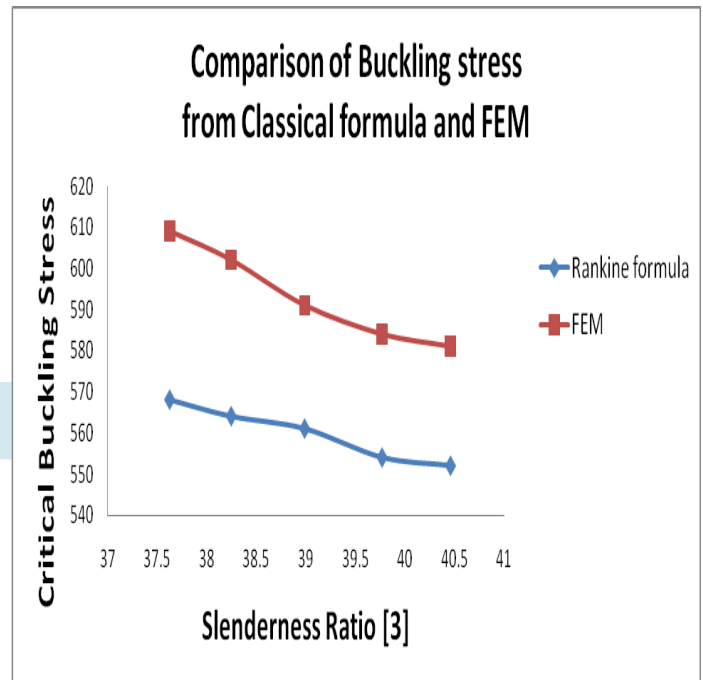


Figure 4.1- Experimental and Simulation Result the Reduced cross section of Connecting rod

Above result shows the validation of present method to determine the buckling stress which is near to the value of classical method of buckling or rankine formula.

#### 4.7 The Calculation of Allowable Stress, Buckling Stress & Factor of Safety

Table 4.2- Simulation Result Allowable stress for the Connecting rod of I-section

Calculation For Factor of Safety					
Thicknes s(L1)	Critical Buckling Stress	Allowable Stress (on compressive force of 64.7KN)			
		Locatio n-1	Locatio n-2	Locatio n-3	Locatio n-4
26	609	196.89	238.33	235.48	271.66
25	602	198.2	244.86	238.49	273.48
24	591	202.68	247.39	241.46	276.66
23	584	207.36	251.66	244.68	279.43
22	581	210.58	253.43	248.88	281.98

Above table and graph shows a validation of experimental result of connecting rod of allowable stresses and factor of safety results and also buckling stress & allowable stress is calculated at various location discussed in previous article no. 4.2 with different width the value of buckling stress & allowable stress of respective location is shown in the table no.4.2 the value will further used to determine the factor of safety at various locations.

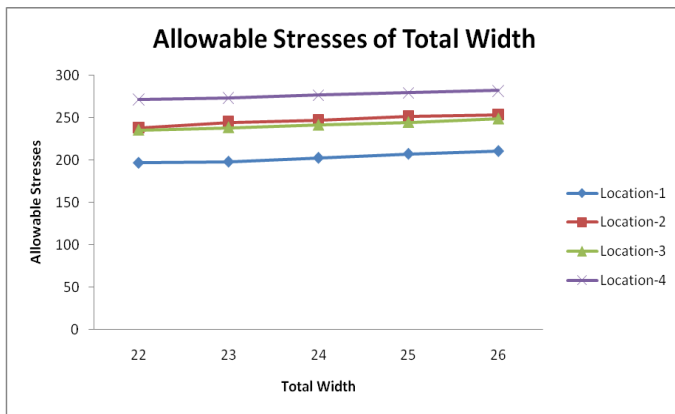


Figure 4.2- Validation of Allowable Stress of I-Cross Section of the Connecting rod

Table 4.3- Validation of experimental result of allowable result of different location of connecting rod

Factor of Safety				
Thickness(L1)	Location -1	Location -2	Location -3	Location -4
26	3.09	2.55	2.58	2.24
25	3.03	2.45	2.52	2.2
24	2.91	2.38	2.44	2.13
23	2.81	2.32	2.38	2.08
22	2.75	2.29	2.33	2.06

The above table shows a Factor of Safety values of different locations of connecting rod at variable thickness from the above results it could be determined that the weak section of connecting rod for further optimization.

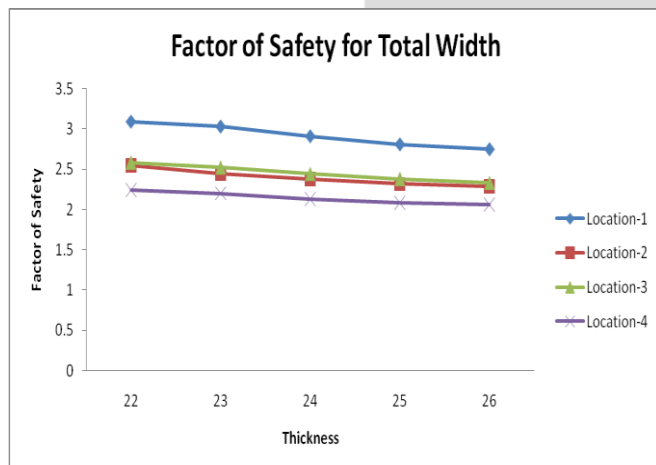


Figure4.3- Validation result of factor of safety of I-Cross Section of the Connecting rod

The graph shows the comparative factor of safety of different locations from the above graph it could be concluded that location no.4 needs to be optimized in future for better strength stability.

#### Optimization Results--

Figure 4.4- Simulation Result Allowable stress for the Connecting rod of optimized-section

Optimized Dimensions		Optimized I -Section					
Middle Thickness(T2)	Side width h (L2)	Thicknes s(L1 )	Critical Bucklin g Stress	Allowable Stress			
				Loc atio n-1	Loc atio n-2	Loc atio n-3	Loc atio n-4
5.5	6	26	614	199 .46	241 .66	237 .84	274 .79
5.4	6.1	25	608	202 .44	247 .8	240 .94	276 .84
5.3	6.2	24	604	205 .49	250 .68	243 .64	279 .7
5.2	6.3	23	596	208 .44	254 .36	246 .86	283 .34
5.1	6.4	22	590	214 .98	256 .79	253 .89	286 .89

Figure 4.5- Reduction rate of cross-sectional area (%) connecting rod of optimized-section

Middle Thickness(T2)	Side Width (L2)	Reduction rate of cross-sectional area (%)
5.5	6	0
5.4	6.1	1.8
5.3	6.2	3.6
5.2	6.3	5.4
5.1	6.4	7.2

Above table shows a reduction rate of cross-sectional area of connecting rod optimized area from this data we are able to predict the reduction on percentage for analysis of allowable stress with respect to middle thickness (T2) and side width (L2).

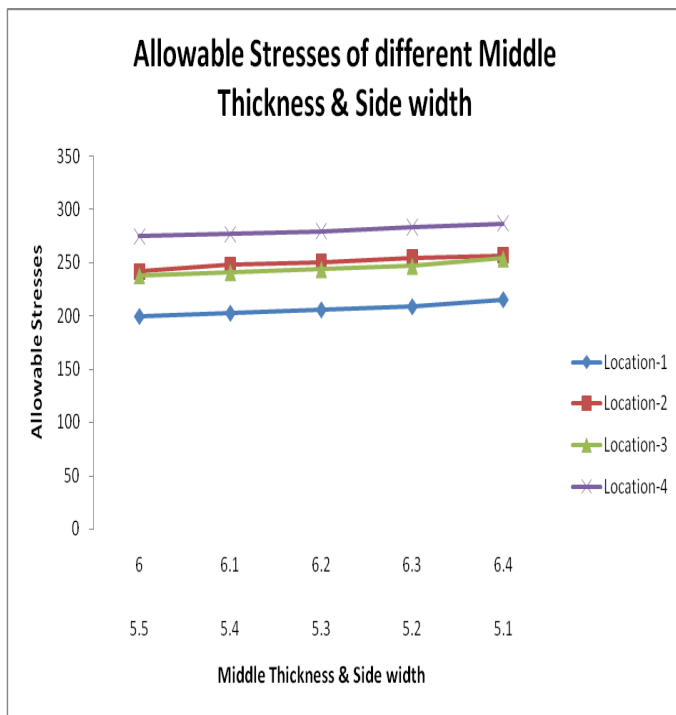


Figure 4.4- Optimization result of Allowable stress of optimized-Cross Section of the Connecting rod of Middle Thickness & Side width

Figure 4.6- Simulation Result Allowable stress for the Connecting rod of Middle Thickness & Side width

Factor of Safety (Optimization)						
Thickn ess(L1)	Middle Thickne ss	Side width h	Loca tion- 1	Loca tion- 2	Loca tion- 3	Loca tion- 4
26	5.5	6	3.07	2.54	2.58	2.23
25	5.4	6.1	3	2.45	2.52	2.19
24	5.3	6.2	2.93	2.4	2.47	2.15
23	5.2	6.3	2.85	2.34	2.41	2.1
22	5.1	6.4	2.74	2.29	2.32	2.05

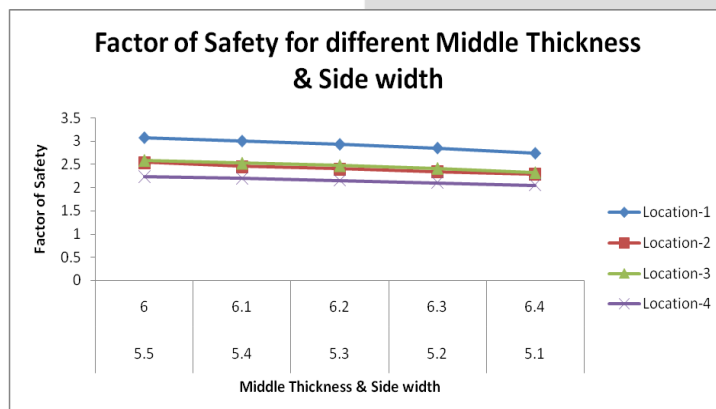


Figure 4.5- Optimization result of Allowable stress of optimized-Cross Section of the Connecting rod of Middle Thickness & Side width

Table-4.7 Simulation Result for the reduced cross section of Connecting rod of I-section and optimized-section

Middle Thickness (T2)	Side width (L2)	Thickn ess(L1)	Ran kin e for mul a	Optimize d cross section	Perce ntage Error
5.5	6	26	568	614	8.1
5.4	6.1	25	564	608	7.8
5.3	6.2	24	561	604	7.7
5.2	6.3	23	554	596	7.6
5.1	6.4	22	552	590	6.9

Above tables and graphs shows an optimization of experimental result of connecting rod of allowable stresses and factor of safety results as well as comparison of Factor of Safety for different Middle Thickness & Side Thickness

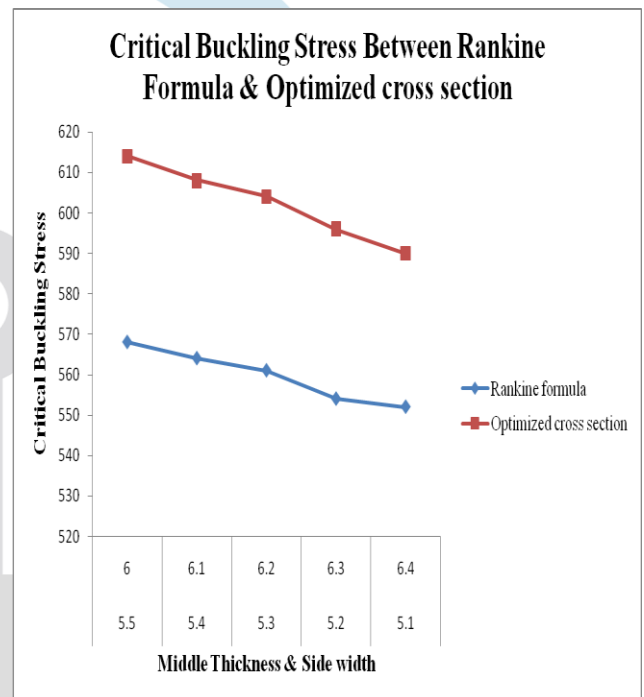


Figure 4.6- Rankine formula and Simulation Result of the optimized cross section of Connecting rod

Above tables and graphs shows an optimization of experimental result of connecting rod of allowable stresses and factor of safety results as well as comparison of critical buckling stress with rankine formula.

## VII. Conclusion:

The current analysis has presented a study of factor of study characteristics of a connecting rod of different profiles. Buckling analysis was carried out on connecting rod of Micro Alloyed Carbon Steel (C70S6) system. The effect of different middle thickness & side width of the connecting rod with middle thickness (5.5, 5.4, 5.3, 5.2, 5.1) & side width (6.0, 6.1, 6.2, 6.3, 6.4) on the factor of safety, critical buckling stress and allowable stress at different location of C70S6 material effects variations along the connecting rod was studied. From the analysis of the results, following conclusions could be drawn.

## REFERENCES

- [1]. H. Grass, C. Krempaszy \*, E. Werner “3-D FEM-simulation of hot forming processes for the production of a connecting rod” Computational Materials Science 36 (2006) 480–489.
- [2]. S. Griza \*, F. Bertoni, G. Zanon, A. Reguly, T.R. Strohaecker “Fatigue in engine connecting rod bolt due to forming laps” Engineering Failure Analysis 16 (2009) 1542–1548.
- [3]. Moon Kyu Lee a, Hyungyi Lee a,\*, Tae Soo Lee a, Hoon Jang b “Buckling sensitivity of a connecting rod to the shank sectional area reduction” Materials and Design 31 (2010) 2796–2803.
- [4]. Liming Zheng, Shuqing Kou, Shenhua Yang, Lili Li, Fei Li “A study of process parameters during pulsed Nd:YAG laser notching of C70S6 fracture splitting connecting rods” Optics & Laser Technology 42 (2010) 985–993.
- [5]. Vanluu Dao, Shengdun Zhao n, Wenjie Lin, Chenyang Zhang “Effect of process parameters on microstructure and mechanical properties in AlSi9Mg connecting-rod fabricated by semi-solid squeeze casting” Materials Science & Engineering A 558 (2012) 95–102.
- [6]. Saharash Khare, O.P. Singh, K. Bapanna Dora, C. Sasun “Spalling investigation of connecting rod” Engineering Failure Analysis 19 (2012) 77–86.
- [7]. Xianghui Meng a,b,n, Youbai Xie a,b “A new numerical analysis for piston skirt–liner system lubrication considering the effects of connecting rod inertia” Tribology International 47 (2012) 235–243.
- [8]. S B Chikalthankar\*, V M Nandedkar\*\*, Surendra Prasad Baratam\* “ Fatigue Numerical Analysis for Connecting Rod” International Journal of Engineering Research and Applications (IJERA) ISSN: 2248-9622.
- [9]. Prof. N.P.Doshi, Prof .N.K.Ingole “Analysis of Connecting Rod Using Analytical and Finite Element Method” International Journal of Modern Engineering Research (IJMER) www.ijmer.com Vol.3, Issue.1, Jan-Feb. 2013 pp-65-68.
- [10]. Bai-yan He a,, Guang-da Shi a, Ji-bing Sun b, Si-zhuan Chen a, Rui Nie a “Crack analysis on the toothed mating surfaces of a diesel engine connecting rod” Engineering Failure Analysis 34 (2013) 443–450.
- [11]. G. Naga Malleshwara Rao “Design Optimization and Analysis of a Connecting Rod using ANSYS” International Journal of Science and Research (IJSR), India Online ISSN: 2319-7064.
- [12]. Leela Krishna Vegi, Venu Gopal Vegi “ Design And Analysis of Connecting Rod Using Forged steel” International Journal of Scientific & Engineering Research, Volume 4, Issue 6, June-2013 ISSN 2229-5518.
- [13]. Y.J. Zhang\*, H.P. Luo, G.X. Liu, Z.N. Guo, Y.J. Tang “Research on power supply and control system of WEDM cutting of stress-notches in fracture splitting processing of connecting rod” Procedia CIRP 6 ( 2013 ) 250 – 254.
- [14]. Kuldeep B1, Arun L.R2, Mohammed Faheem3 “Analysis And Optimization Of Connecting Rod Using Alfasic Composites” International Journal of Innovative Research in Science, Engineering and Technology Vol. 2, Issue 6, June 2013.
- [15]. Ling Li ↑, Rong Wang “Failure analysis on fracture of worm gear connecting bolts” Engineering Failure Analysis 36 (2014) 439–446.
- [16]. Weijun HUI 1, Silian CHEN 2, Chengwei SHAO 1, Yongjian ZHANG 1, Han DONG 2 “Hot Deformation Behavior of Vanadium micro alloyed Medium carbon Steel for Fracture Splitting Connecting Rod” JOURNAL OF IRON AND STEEL RESEARCH, INTERNATIONAL □ 2 0 1 5, 2 2 ( 7 ): 6 1 5 G 6 2 1.
- [17]. Mr. J.D.Ramani\*, Prof. Sunil Shukla\*\*, Dr. Pushpendra Kumar Sharma “FE-Analysis of Connecting Rod of I.C.Engine by Using Ansys for Material Optimization” Mr. J.D.Ramani et al Int. Journal of Engineering Research and Applications www.ijera.com ISSN : 2248-9622, Vol. 4, Issue 3 (Version 1), March 2014, pp.216-220.
- [18]. Mohammed Mohsin Ali Ha, Mohamed Haneef b\* “Analysis of Fatigue Stresses on Connecting Rod Subjected to Concentrated Loads At The Big End” Materials Today: Proceedings 2 ( 2015 ) 2094 – 2103.
- [19]. J.P. Fuertes, O. Murillo, J. Leóna,\*, C. Luisa, D. Salcedo, I. Puertasa, R. Luria “Mechanical properties analysis of an Al-Mg alloy connecting rod with submicrometric structure” Procedia Engineering 132 ( 2015 ) 313 – 318.
- [20]. D.Gopinatha, Ch.V.Sushma\* “Design and Optimization of Four Wheeler Connecting Rod Using Finite Element Analysis” Materials Today: Proceedings 2 ( 2015 ) 2291 – 2299.
- [21]. He Zhenpeng et.al. “Tribological performances of connecting rod and by using orthogonal experiment, regression method and response surface methodology” <http://dx.doi.org/10.1016/j.asoc.2015.01.009>.
- [22]. Yu Wang a, Feng-Ming Li a “Nonlinear dynamics modeling and analysis of two rods

connected by a joint with clearance”  
<http://dx.doi.org/10.1016/j.apm.2014.10.056>.

- [23]. Puran Singh<sup>1</sup>, Debashis Pramanik<sup>2</sup>, Ran Vijay Singh<sup>3</sup> “Fatigue and Structural Analysis of Connecting Rod’s Material Due to (C.I) Using FEA” International Journal of Automotive Engineering and Technologies Vol. 4, Issue 4, pp. 245– 253,2015.
- [24]. J.P. Fuertes<sup>1</sup>, C.J. Luis<sup>2</sup>, R. Luri<sup>3</sup>, D. Salcedo<sup>4</sup>, J. León<sup>5</sup>, I. Puertas<sup>\*</sup>,<sup>6</sup> “Design, simulation and manufacturing of a connecting rod from ultra-fine grained material and isothermal forging” Journal of Manufacturing Processes 21 (2016) 56–68.
- [25]. C. Juarez a, F.Rumiche a,<sup>\*</sup>, A.Rozas a, J.Cuisano b, P.Lean b “Failure analysis of a diesel generator connecting rod” Case Studies in Engineering Failure Analysis 7 (2016) 2

